THE JOURNAL OF BIOLOGICAL CHEMISTRY VOL. 286, NO. 39, pp. 33845–33853, September 30, 2011
Printed in the U.S.A.

Human Mre11/Human Rad50/Nbs1 and DNA Ligase IIIα/XRCC1 Protein Complexes Act Together in an Alternative Nonhomologous End Joining Pathway*[S]

Received for publication, June 20, 2011, and in revised form, July 30, 2011 Published, JBC Papers in Press, August 3, 2011, DOI 10.1074/jbc.M111.274159

Julie Della-Maria[‡], Yi Zhou[§], Miaw-Sheue Tsai[¶], Jeff Kuhnlein[§], James P. Carney[‡1], Tanya T. Paull[§], and Alan E. Tomkinson[‡‖2]

From the [‡]Radiation Oncology Research Laboratory, Department of Radiation Oncology and The Marlene and Stewart Greenebaum Cancer Center, University of Maryland School of Medicine, Baltimore, Maryland 21201, the [¶]Ernest Lawrence Berkeley National Laboratory, University of California, Berkeley, California 94720, the [§]Howard Hughes Medical Institute and the Department of Molecular Genetics and Microbiology, University of Texas, Austin, Texas 78712, and the [‖]Department of Internal Medicine and University of New Mexico Cancer Center, University of New Mexico, Albuquerque, New Mexico 87131

Recent studies have implicated a poorly defined alternative pathway of nonhomologous end joining (alt-NHEJ) in the generation of large deletions and chromosomal translocations that are frequently observed in cancer cells. Here, we describe an interaction between two factors, hMre11/hRad50/Nbs1 (MRN) and DNA ligase IIIα/XRCC1, that have been linked with alt-NHEJ. Expression of DNA ligase IIIα and the association between MRN and DNA ligase IIIα/XRCC1 are altered in cell lines defective in the major NHEJ pathway. Most notably, DNA damage induced the association of these factors in DNA ligase IV-deficient cells. MRN interacts with DNA ligase IIIα/XRCC1, stimulating intermolecular ligation, and together these proteins join incompatible DNA ends in a reaction that mimics alt-NHEJ. Thus, our results provide novel mechanistic insights into the alt-NHEJ pathway that not only contributes to genome instability in cancer cells but may also be a therapeutic target.

The repair of DNA double-strand breaks (DSBs)[3] is of the utmost importance for cell viability and genomic stability. Notably, defects in DSB repair result in genomic rearrangements that promote cancer formation and progression (1–3). Although there are multiple DSB repair pathways, these pathways can be divided into two groups depending on whether the repair reaction is dependent or not upon substantial DNA sequence homology between the recombining molecules (4, 5). The key step of the major homology-dependent pathway is the invasion of a single strand into a homologous duplex. In contrast, the key step of nonhomologous end joining (NHEJ) involves the end-to-end alignment of broken DNA molecules (4, 5).

Unlike the major homology-dependent pathway, repair of DSBs by the major or classic NHEJ (C-NHEJ) pathway is error-prone, frequently resulting in the loss or addition of a few nucleotides at the break site (4, 5). Despite the mutagenic consequences of NHEJ, this is a major DSB repair pathway in mammalian cells. In addition, there is emerging evidence for alternative versions of NHEJ (alt-NHEJs) that are more error-prone than C-NHEJ. Although alt-NHEJ is more evident in cells that are deficient in C-NHEJ (6, 7), it is detectable in wild-type cells (8). Repair of DSBs by alt-NHEJ is characterized by the presence of short tracts of sequence homology (microhomologies) at the repair site, large deletions, and chromosome translocations (6–10). Furthermore, alt-NHEJ appears to be responsible for chromosomal translocations found in cancer cells (11–15) and to make a much greater contribution to DSB repair in cancer cells compared with normal cells (10).

A combination of biochemical and molecular genetic studies by many laboratories has identified the key components of C-NHEJ (4, 5). In contrast, the factors involved in and the mechanisms of alt-NHEJ are not well defined. Poly(ADP-ribose) polymerase-1 (PARP-1), the initiating protein for DNA single-strand break (SSB) repair, also binds to DSBs (16) and has been implicated in DNA PK-independent NHEJ (17, 18). The hMre11/hRad50/Nbs1 (MRN) complex, which is an early participant in cell cycle checkpoint pathways activated by DSBs and is involved in the end resection step in recombinational repair of DSBs (19, 20), also plays a role in alt-NHEJ (21–24). DNA ligase IIIα/XRCC1, which is targeted to SSBs by an interaction with poly(ADP-ribosylated) PARP-1 (25, 26), appears to be involved in the completion of DSB repair by alt-NHEJ (10, 17, 27, 28). In this study, we demonstrate that DNA ligase IIIα/XRCC1 and MRN are constitutively associated in undamaged wild-type cells but dissociate in response to DNA damage. However, in cell lines that are defective in C-NHEJ, the steady-state levels of DNA ligase IIIα are elevated, and the association

* This work was supported, in whole or in part, by National Institutes of Health (NIH) Grant ES012512 from the NIEHS (to A. E. T.), NIH Program Project Grant CA92584 from the NCI (to A. E. T. and T. T. P.), and NIH Grant CA094008 (to T. T. P.).

[S] The on-line version of this article (available at http://www.jbc.org) contains supplemental Figs. S1 and S2.

[1] Present address: Battelle, Edgewood Chemical Biological Center, AMSRD-ECB-RT-BM, Bldg. E3831, 5183 Blackhawk Rd., Aberdeen Proving Ground, MD 21010.

[2] To whom correspondence should be addressed: Cancer Research Facility, 915 Camino de Salud, 1 University of New Mexico, Albuquerque, NM 87131. Tel.: 505-272-5404; E-mail: atomkinson@salud.unm.edu.

[3] The abbreviations used are: DSB, double-strand break; ATM, ataxia telangiectasia mutated; ATR, ataxia telangiectasia and Rad3 related; BRCT, breast cancer susceptibility protein 1 C-terminal domain; NHEJ, nonhomologous end joining; alt-NHEJ, alternative version of NHEJ; C-NHEJ, classic NHEJ; FHA, forkhead-associated; MRN, hMre11/hRad50/Nbs1; PARP-1, poly(ADP-ribose) polymerase-1; SSB, single-strand break; XRCC1, X-ray repair cross-complementing protein 1.

between DNA ligase IIIα/XRCC1 and MRN is abnormal, suggesting that these factors act together in alt-NHEJ. In support of this idea, we show that DNA ligase IIIα/XRCC1 and MRN physically and functionally interact to join DNA ends in a reaction that mimics alt-NHEJ.

EXPERIMENTAL PROCEDURES

Cell Culture—The human pre-B cell line Nalm6 and its *lig4*-null derivative N114P2 were cultured as described (29). The DNA ligase IV mutant cell line LB 2304, derived from patient 2304 (1738C>T (R580X) and 2440C>T (R814X) giving truncated proteins) and a wild-type (NC-10) human lymphoblastoid cell line were cultured in RPMI 1640 medium supplemented with 15% fetal calf serum, 10 units/ml penicillin, 10 μg/ml streptomycin, and 2 mM glutamine or 1 mM sodium pyruvate, respectively (Cellgro) (30). The DNA PK-proficient and -deficient human glioblastoma cell lines, MO59J and MO59K were cultured as described (31). HeLa cells were cultured in DMEM supplemented with 10% FBS, 10 units/ml penicillin, and 10 μg/ml streptomycin (Invitrogen). When indicated, cells were preincubated for 30 min with the DNA PK inhibitor LY294,002 (200 μM; Sigma).

Immunoprecipitation—Cells ($1–3 \times 10^7$) were either mock treated or irradiated (10 grays) and then allowed to recover for 1 h. Nuclear extracts were prepared as described previously (32). Proteins A/G-Sepharose beads (20 μl each) were incubated with a hMre11 monoclonal antibody (3–5 μl; GeneTex) and 45 to 100 μg of nuclear extract in 1 ml of 20 mM HEPES-KOH (pH 7.8), 150 mM NaCl, 0.1% Igepal CA-630 (Sigma), 10% glycerol, 1 mM DTT containing a mixture of protease inhibitors for 16 h at 4 °C. After washing, bound proteins were eluted with SDS loading buffer and detected by immunoblotting after separation by SDS-PAGE. To detect multiple proteins, membranes were stripped in PBS containing 2% SDS and 0.1 M β-mercaptoethanol for 30 min, washed with PBS for 30 min, and reprobed with a different antibody.

Purification of the MRN Complex and Subcomplexes—The hMre11 mutant H129L/D130V was made in pTP813 (33), which contains the hMre11 cDNA with a C-terminal FLAG epitope tag by a QuikChange mutagenesis using primers TP255 (5′-CAGTGTTTAGTATTCATGGCAATCTTGTCG-ATCCCACAGGGGCAGATGCACTTTGTGC-3′) and its complement TP256, to yield the baculovirus transfer vector pTP2196 and the corresponding bacmid pTP2197. This was used to make baculovirus according to manufacturer's instructions (Invitrogen). Wild-type and H129L/D130V mutant MR complexes were expressed in Sf21 insect cells using the method described previously for MRN (33). For the experiments shown here, FLAG-tagged Nbs1 was expressed and purified separately using the baculovirus transfer vector pTP288 (bacmid is pTP289) as described previously (34). hMre11, hMre11/hRad50, and hMre11/Nbs1 were purified from baculovirus-infected insect cells as described (35, 36).

Pulldown Assays—Glutathione-Sepharose beads (30 μl; Amersham Biosciences) liganded by either GST-DNA ligase IIIβ or GST (2 μg of each) were incubated for 1 h at 4 °C with MRN, MR, MN, or hMre11 (3 nM each) in 50 mM Tris-HCl (pH 7.5), 150 mM NaCl, 5 mM EDTA, 0.1% Igepal CA-630, and 5% BSA. After washing, bound proteins were eluted with SDS loading buffer and detected by immunoblotting with hMre11 (GeneTex), Nbs1 (Novus), and hRad50 antibodies (37) after separation by SDS-PAGE. In similar assays, GST-DNA ligase IIIβ and GST beads were incubated with truncated derivatives of Nbs1 lacking either the forkhead-associated (FHA) domain or BRCT domain that had been labeled by coupled *in vitro* transcription and translation (TNT7 kit; Promega). Labeled polypeptides retained by the GST beads were detected by phosphorimaging after separation by SDS-PAGE.

Yeast Two-hybrid Assay—Full-length versions of DNA ligase IIIα and DNA ligase IIIβ (38) were amplified by the PCR and then subcloned into the plasmid pGBK to generate GAL4 DNA binding domain fusion proteins. Full-length Nbs1 and truncated versions lacking either the BRCT domain alone or both the FHA and BRCT domains, and a version containing only the FHA domain were subcloned into the plasmid pGADT7 to generate GAL4 activation domain fusion proteins. Derivatives of pGBK and pGADT7 were transformed individually into the isogenic haploid yeast strains PJ69-4α and PJ69-4a, respectively. Protein-protein interactions were screened as described previously (39).

Expression and Purification of the DNA Ligase IIIα/XRCC1 Complex—Full-length versions of DNA ligase IIIα and XRCC1 were subcloned into the plasmid pFastBac to generate the plasmids pFastBac-LigIIIα and pFastBac-XRCC1. After verification by DNA sequencing, the pFastBac plasmids were transformed into *Escherichia coli* DH10Bac cells containing the bacmid (Invitrogen) to generate baculoviruses encoding either DNA ligase IIIα or XRCC1. Suspension cultures of SF9 insect cells (0.9 liter) were co-infected with the DNA ligase IIIα and XRCC1 baculoviruses at a multiplicity of infection of 10:1 and 20:1, respectively. Cells were harvested 72 h after infection and, after resuspension in 50 mM NaH_2PO_4, 10 mM Tris-HCl (pH 8.0), 300 mM NaCl, and 0.5% Igepal CA-630 containing a mixture of protease inhibitors, lysed by sonication. The DNA ligase IIIα/XRCC1 complex was purified from the clarified extract by sequential phosphocellulose, Hi-Trap SP-Sepharose, Superdex 200, Mono Q, and Mono S (Amersham Biosciences) column chromatography steps. Approximately 1 mg of >98% homogeneous DNA ligase IIIα/XRCC1 was obtained from the 0.9-liter culture.

Ligation Assays—DNA concentrations are expressed as DNA ends. A linear duplex DNA fragment (580 bp) with 3′-complementary single-strand ends was generated by digestion of the pGADT7 vector (Clontech) with PstI. Ligation reactions were carried out using 2 pmol of substrate, 400 fmol to 1.6 pmol of DNA ligase IIIα/XRCC1, and 400 fmol, 800 fmol, and 1.2 pmol of MRN as indicated, in 60 mM Tris-HCl (pH 7.5), 10 mM $MgCl_2$, 5 mM DTT, 1 mM ATP, and 50 μg/ml BSA at 30 °C for 1 h. After incubation with proteinase K at 37 °C for 1 h, DNA molecules in the reactions were separated by electrophoresis on a 1% agarose gel and then stained with ethidium bromide. Ligation was quantified using the Quantity One software (Bio-Rad).

Longer DNA substrates were made by digesting pCDF-1b plasmid (Novagen) with PstI to generate a 3621-bp substrate with 3′-complementary single-strand ends or with BglI and EcoNI to generate a 2915-bp substrate with incompatible, non-

palindromic ends. The ligation reaction was performed in a 10-μl mixture containing 5 mM $MgCl_2$, 60 mM NaCl, 25 mM MOPS (pH 7.0), 1 mM DTT, 1 mM ATP, 50 μg/ml BSA, DNA substrate (16 fmol for compatible DNA substrate, 20 fmol for incompatible DNA substrate), and the indicated protein. The mixture was preincubated at 37 °C for 10 min, followed by the addition of DNA ligase IIIα/XRCC1 (1.4 fmol for compatible DNA substrate, 180 fmol for incompatible DNA substrate) and further incubation at 37 °C for 10 min (compatible DNA) or 30 min (incompatible DNA). The reaction was stopped by adding 1 μl of 2% SDS, 100 mM EDTA and deproteinized with proteinase K at 37 °C for 30 min. The samples were then used for electrophoresis on a 0.7% native agarose gel. DNA was visualized using SYBR Green (Invitrogen) on a Typhoon imager (GE Healthcare), and the ligation products were quantified using ImageQuant TL version 2005 software.

Analysis of Junctions Generated by Joining of Incompatible DNA Ends—Linear DNA molecules were generated by digestion of pGADT7 (Invitrogen) with BamHI and EcoRI for the four nucleotide 5′ overhangs and of pcDNA4HisMax C (Invitrogen) with KpnI and PstI for the four nucleotide 3′ overhangs. Intramolecular joining of the incompatible ends was carried out in 25 mM MOPS (pH 7.0), 60 mM KCl, 0.2% Tween 20, 2 mM DTT, 4 mM $MgCl_2$, 2 mM $MnCl_2$, 0.5 mM ATP, 0.8 pmol of plasmid DNA, 10% polyethylene glycol, 0.01 pmol of DNA ligase III/XRCC1 or DNA ligase IV/XRCC4, and 0.06 pmol of hMre11 or MRN as indicated, in a volume of 10 μl. After incubation at 37 °C for 25 min, Tween 20 was added to a final concentration of 0.5%, and a 2.5-μl aliquot was amplified by PCR using the MATCHMAKER 5′ and 3′ AD LD-Insert Screening Amplimers (20 ng; Clontech) and *Pfu* DNA polymerase (0.5 unit; Stratagene) in a 20 μl reaction mixture containing 2 μl of 10 × Cloned Pfu DNA Polymerase buffer (Stratagene) and dNTPs (200 μM each). The PCR conditions were 94 °C for 30 s followed by 30 cycles at 94 °C for 15 s, 55 °C for 30 s, and 72 °C for 30 s, and then a 10-min extension at 72 °C. PCR products were cloned using the TOPO-TA cloning kit (Invitrogen) as described by the manufacturer and sequenced.

RESULTS

Association of MRN and DNA Ligase IIIα in Normal and DNA Ligase IV-deficient Cells—Because alt-NHEJ is more evident in cells that are deficient in C-NHEJ (6, 7), we asked whether reduction of DNA ligase IV activity alters the behavior of two DNA repair factors, MRN and DNA ligase IIIα/XRCC1, that have been implicated in alt-NHEJ. In a pre-B cell line, Nalm6 (Fig. 1*A*) and a lymphoblastoid cell line, NC10 (Fig. 1*B*), established from normal individuals, MRN and DNA ligase IIIα/XRCC1 were constitutively associated in undamaged cells but dissociated in response to ionizing radiation. Similar results were obtained with HeLa cells (Fig. 2*B*) and when the immunoprecipitation was carried out in the presence of ethidium bromide (data not shown).

In the *lig4*-null N114P2 cells (supplemental Fig. S1), the steady-state levels of DNA ligase IIIα are about 2-fold higher than in the wild-type parental Nalm6 cells (Fig. 1*A*, *left*). Similarly, the lymphoblastoid cell line, LB 2304, established from a DNA ligase IV-deficient individual (supplemental Fig. S1), has higher steady-state levels of DNA ligase IIIα than a comparable cell line from a normal individual (Fig. 1*B*, *left*). Despite the elevated steady-state levels of DNA ligase IIIα in DNA ligase IV-deficient cells (Fig. 1), the amount of DNA ligase IIIα constitutively associated with MRN was much lower than in comparable wild-type cells (Fig. 1). More strikingly, there was a dramatic increase in the amount of DNA ligase IIIα associated

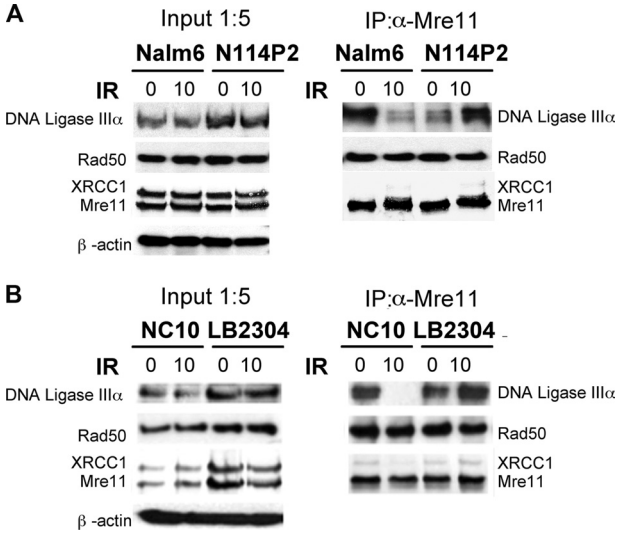

FIGURE 1. **DNA damage induced association of DNA ligase IIIα/XRCC1 and MRN in DNA ligase IV-deficient cells.** Nuclear extracts were prepared from wild-type human pre-B cell line, Nalm6 and its *lig4*-null derivative, N114P2 (*A*) or wild-type human lymphoblastoid cell line, NC10, and DNA ligase IV mutant lymphoblastoid cell line, LB2304 (*B*), that had been either mock treated (*0*) or treated with γ-irradiation (*IR*, 10 grays). *Left*, proteins in the nuclear extracts (*Input 1:5*, 20 μg) were detected by immunoblotting with the indicated antibodies. *Right*, nuclear extracts (100 μg) were incubated with hMre11 antibody (*IP*: α-Mre11), and proteins in the immunoprecipitates were detected by immunoblotting.

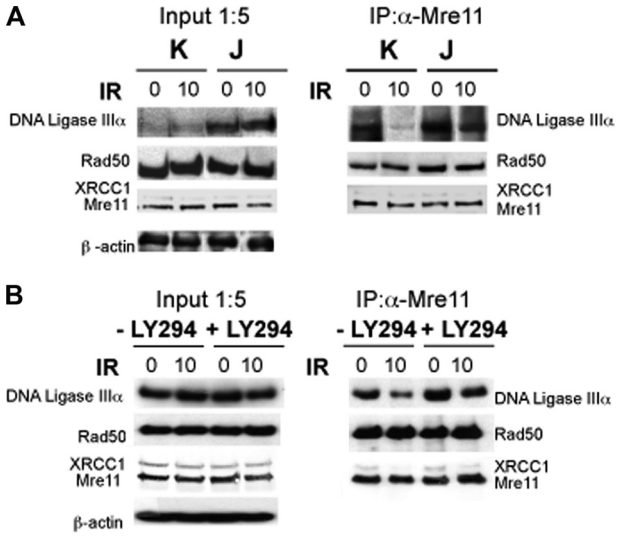

FIGURE 2. **Effect of DNA PK activity on DNA damage-dependent dissociation of DNA ligase IIIα and MRN.** Nuclear extracts were prepared from DNA-PK-deficient, MO59J, and DNA PK-proficient, MO59K, glioblastoma cells (*A*, 45 μg) or HeLa cells (60 μg) (*B*) that had been either mock-treated (*0*) or treated with γ-irradiation (*IR*, 10 grays). Where indicated, cells were incubated without (−LY294) or with 200 μM LY294,002 (+LY294) for 30 min prior to irradiation. *Left*, proteins in the nuclear extracts (*Input 1:5*) were detected by immunoblotting with the indicated antibodies. *Right*, nuclear extracts were incubated with hMre11 antibody (*IP*: α-Mre11), and proteins in the immunoprecipitates were detected by immunoblotting.

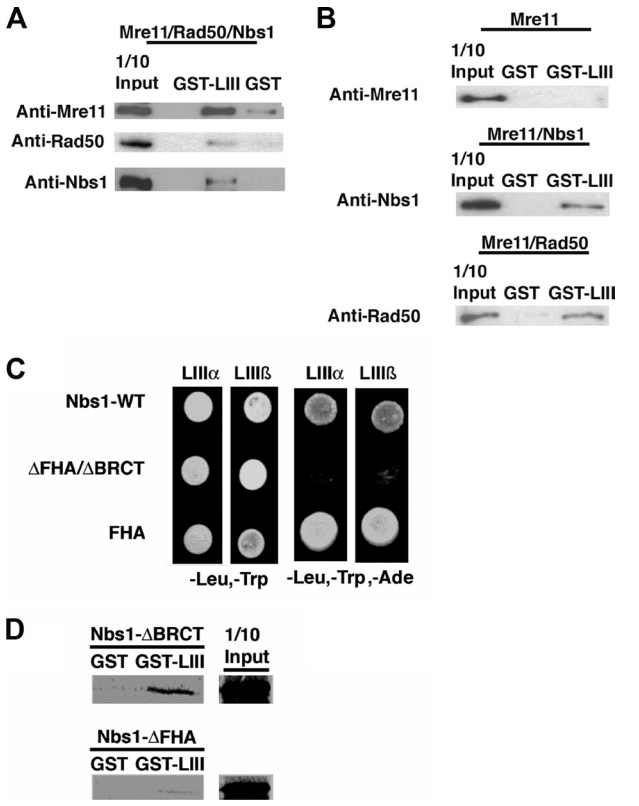

FIGURE 3. **Mapping the interacting regions of MRN and DNA ligase IIIα.** *A* and *B*, pulldown assays performed using glutathione beads liganded by either GST (2 μg) or GST-DNA ligase IIIβ (GST-LigIII, 2 μg) and purified human MRN (3 nM), purified hMre11, hMre11/hRad50, or hMre11/Nbs1 (3 nM each) as indicated. Binding was detected by immunoblotting using the indicated antibodies. C, interactions of full-length Nbs1 and truncated derivatives with DNA ligase IIIα and β using the yeast two-hybrid assay. *D*, binding of labeled *in vitro* translated derivatives of Nbs1 lacking either the BRCT (*upper*) or FHA domain (*lower*) to glutathione beads liganded by either GST (2 μg) or GST-DNA ligase IIIβ (GST-LigIII, 2 μg).

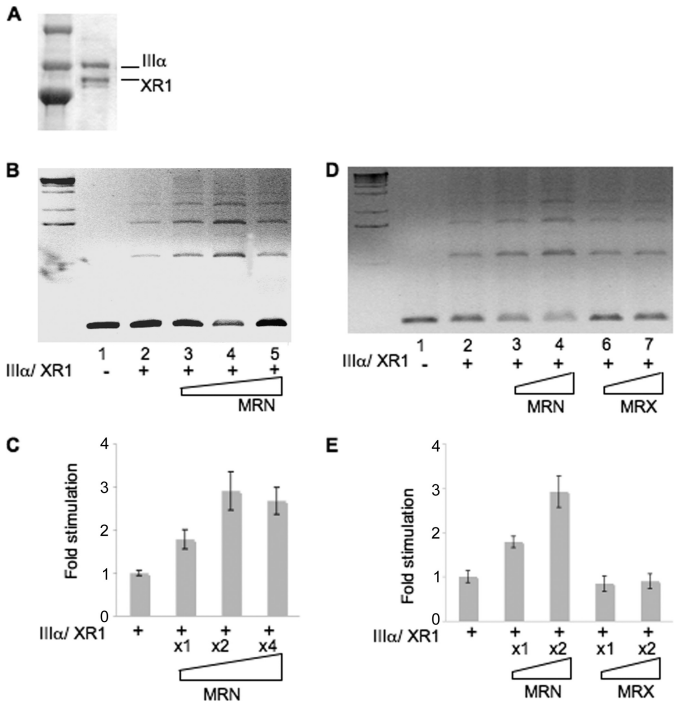

FIGURE 4. **MRN stimulates intermolecular ligation by DNA ligase IIIα/XRCC1.** *A*, Coomassie Blue-stained gel of purified DNA ligase IIIα/XRCC1 (150 ng). *B*, linear 580-bp DNA molecules with cohesive four-nucleotide 3′ overhangs (*lane 1*, 2 pmol) incubated with: DNA ligase IIIα/XRCC1 (400 fmol) and no addition (*lane 2*), 400 fmol of human MRN (*lane 3*), 800 fmol of human MRN (*lane 4*), 1.2 pmol of human MRN (*lane 5*). *C*, graphic representation of the DNA joining assay shown in *B*. The results of three independent experiments after quantification with the Quantity One software (Bio-Rad) are expressed as increase in DNA joining compared with reactions with DNA ligase IIIα/XRCC1 alone. *Error bars* indicate S.D. *D*, linear 580-bp DNA molecules with cohesive four-nucleotide 3′ overhangs (*lane 1*, 1.2 pmol) incubated with DNA ligase IIIα/XRCC1 (400 fmol) and no addition (*lane 2*), 400 fmol of human MRN and yeast MRX (*lanes 3* and *6*, respectively), 800 fmol of human MRN and yeast MRX (*lanes 4* and *7*, respectively). *E*, graphic representation of the DNA joining assay shown in *D*. The results of three independent experiments after quantification with the Quantity One software (Bio-Rad) are expressed as increase in DNA joining compared with reactions with DNA ligase IIIα/XRCC1 alone. *Error bars* indicate S.D.

with MRN following DNA damage, suggesting that these factors participate together in a repair pathway that compensates for reduced C-NHEJ (Fig. 1).

Effect of DNA PK Activity on the Association between MRN and DNA Ligase IIIα—To determine whether the altered association of MRN and DNA ligase IIIα/XRCC1 is a common feature of cells that are defective in C-NHEJ, we utilized a pair of cell lines M059K and M059J established from a human glioblastoma that are DNA PK-proficient and -deficient (31), respectively. The steady-state level of DNA ligase IIIα was significantly higher (about 8-fold) and more DNA ligase IIIα was associated with MRN in the absence of DNA damage in the DNA PK-deficient cells compared with the DNA PK-proficient cells (Fig. 2*A*).

Because the DNA PK mutant cells are also ATM-defective (40), the contribution of DNA PK deficiency to the altered behavior of DNA ligase IIIα/XRCC1 cannot be definitively determined in these cells. To examine more directly the role of DNA PK in the DNA damage-induced dissociation of MRN and DNA ligase IIIα/XRCC1, we carried out studies with the PI3 kinase inhibitor LY294,002 that inhibits DNA PK but not ATM or ATR at 200 μM (41). As expected, incubation of HeLa cells with the DNA PK inhibitor for 30 min did not result in significant changes in the steady-state levels of MRN and DNA ligase IIIα/XRCC1, but there was an approximately 1.5-fold increase in the amount DNA ligase IIIα associated with MRN in undamaged cells (Fig. 2*B*). Moreover, although the DNA PK inhibitor did not prevent the DNA damage-induced dissociation of MRN and DNA ligase IIIα/XRCC1, significantly more DNA ligase IIIα remained associated MRN in extracts from cells treated with the DNA PK inhibitor (Fig. 2*B*). Because similar results were obtained with the DNA PK inhibitor and the DNA PK mutant cell line, it appears that DNA PK activity contributes to but is not required for the dissociation of MRN and DNA ligase IIIα/XRCC1 in undamaged cells and following DNA damage.

Physical Interaction between the MRN and DNA Ligase IIIα/XRCC1 Complexes—The elevated steady-state levels of DNA ligase IIIα and the increased association with MRN following DNA damage in cells that are defective in C-NHEJ are consistent with these factors acting together in the repair of DSBs by alt-NHEJ. To determine whether MRN and DNA ligase IIIα/XRCC1 interact directly, we performed pulldown assays with the purified complexes. hRad50 and the other subunits of the MRN complex bound specifically to beads liganded by DNA ligase IIIβ (Fig. 3*A*), a germ cell-specific form of DNA ligase

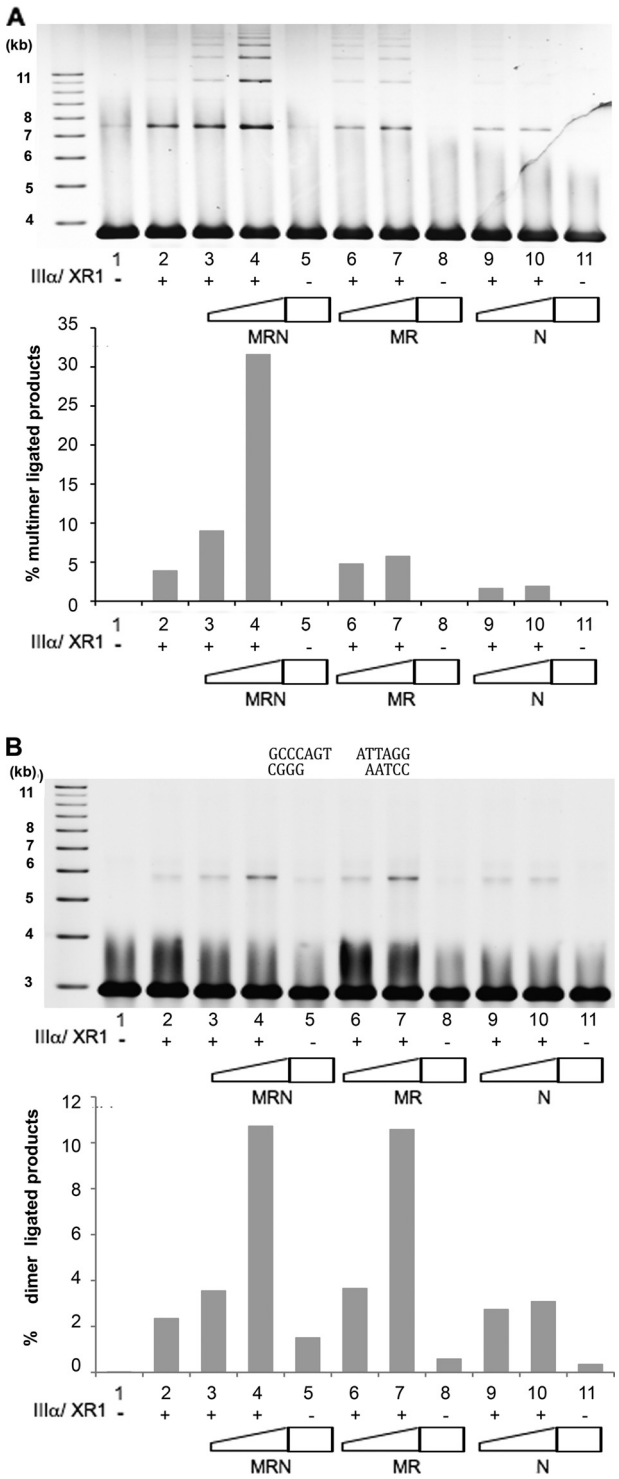

FIGURE 5. **MRN stimulates compatible and incompatible DNA end ligation by DNA ligase IIIα/XRCC1.** *A*, linear plasmid DNA (*lane 1*, 16 fmol) with compatible ends (PstI) was incubated with 1.4 fmol of DNA ligase IIIα/XRCC1 in the presence of no addition (*lane 2*), 312.5 fmol of MRN (*lane 3*), 625 fmol of MRN (*lane 4*), 312.5 fmol of MR (*lane 6*), 625 fmol of MR (*lane 7*), 425 fmol of Nbs1 (*lane 9*), 850 fmol of Nbs1 (*lane 10*). *Lane 5*, 625 fmol of MRN; *lane 8*, 625 fmol of MR, and *lane 11*, 850 fmol of Nbs1. DNA bands were quantified using ImageQuant TL version 2005 software, and the amount of multimeric ligated products was calculated as a percentage of the total DNA in the reaction. *B*, linear plasmid DNA (*lane 1*, 20 fmol) with incompatible, nonpalindromic ends (BglI and EcoNI) was incubated with 180 fmol of DNA ligase IIIα/XRCC1 in the presence of no addition (*lane 2*), 1.25 pmol of MRN (*lane 3*), 1.25 pmol of MRN (*lane 4*), 625 fmol of MR (*lane 6*), 1.25 pmol of MR (*lane 7*), 850 fmol of Nbs1 (*lane 9*), 1.7 pmol of Nbs1 (*lane 10*). *Lane 5*, 1.25 pmol of MRN; *lane 8*, 1.25 pmol of MR; and *lane 11*, 1.7 pmol of Nbs1. DNA bands were quantified, and the percentage of ligation product was calculated as a percentage of the total DNA in the reaction.

III that does not interact with XRCC1 (38). To identify which subunits of the MRN complex interact with DNA ligase IIIβ, we performed similar assays with purified hMre11/hRad50, hMre11/Nbs1, and hMre11 (Fig. 3*B*). The binding of the hMre11/hRad50 and hMre11/Nbs1 subcomplexes but not hMre11 alone suggests that DNA ligase IIIβ interacts with both the hRad50 and Nbs1 subunits of MRN.

In the yeast two-hybrid assay, full-length Nbs1 and a truncated version containing just the N-terminal FHA domain interacted with both DNA ligase IIIα and DNA ligase IIIβ whereas a truncated version of Nbs1 lacking both the FHA and BRCT domains did not (Fig. 3*C*). To provide further evidence that the Nbs1 FHA domain mediates the interaction with DNA ligase III, we performed pulldown assays with labeled *in vitro* translated versions of Nbs1 either lacking the BRCT domain (Fig. 3*D*, *upper*) or lacking the FHA domain (Fig. 3*D*, *lower*). As expected, the polypeptide without the FHA domain was not retained by the DNA ligase IIIβ beads whereas the polypeptide lacking the BRCT domain was. In similar studies, we mapped the region of DNA ligase III that interacts with Nbs1 FHA domain to the N-terminal 390 amino acids (data not shown) that is not required for catalytic activity but contains the DNA-binding zinc finger motif (42).

Effect of MRN on the Joining of Compatible and Incompatible Ends by DNA Ligase IIIα/XRCC1—Because Mre11/Rad50/Xrs2 (MRX), the yeast homolog of MRN, stimulates intermolecular DNA joining by Dnl4/Lif1 (43), we examined the effect of MRN on the DNA joining activity of purified DNA ligase IIIα/XRCC1 (Fig. 4*A*). Unlike Dnl4/Lif1 (43), DNA ligase IIIα/XRCC1 preferentially catalyzed intermolecular rather than intramolecular joining of a 580-bp linear DNA substrate (Fig. 4*B*, *lane 2*). MRN at a 1:1 and 2:1 ratio relative to DNA ligase IIIα/XRCC1 increased intermolecular ligation 1.8- and 2.9-fold, respectively (Fig. 4, *B* and *C*). Because yeast MRX did not stimulate DNA ligase IIIα/XRCC1 activity (Fig. 4, *D* and *E*), the stimulation of DNA ligase IIIα/XRCC1 by MRN is species-specific and so is likely to be a consequence of a protein-protein interaction rather than an effect on the DNA substrate. Under similar conditions, MRX stimulated the intermolecular joining of blunt ends, although ligation of the blunt ends was less efficient (data not shown).

Using longer DNA substrates, we compared the effect of MRN, MR, Nbs1, and hMre11 on the joining of compatible and incompatible DNA ends by DNA ligase IIIα/XRCC1. As expected, MRN markedly enhanced intermolecular joining of compatible DNA ends (Fig. 5*A*, compare *lane 2* with *lanes 3* and *4*). In contrast, MR (Fig. 5*A*, *lanes 6* and *7*), Nbs1 (Fig. 5*A*, *lanes 9* and *10*), and hMre11 (data not shown) did not. Surprisingly, DNA ligase IIIα/XRCC1 had weak but detectable activity on a DNA substrate with incompatible DNA ends (Fig. 5*B*, *lane 2*) that presumably reflects the ability of DNA ligase IIIα/XRCC1 to join mismatched termini (44). Both MRN (Fig. 5*B*, compare *lanes 2* and *4*) and MR (Fig. 5*B*, compare *lanes 2* and *7*)

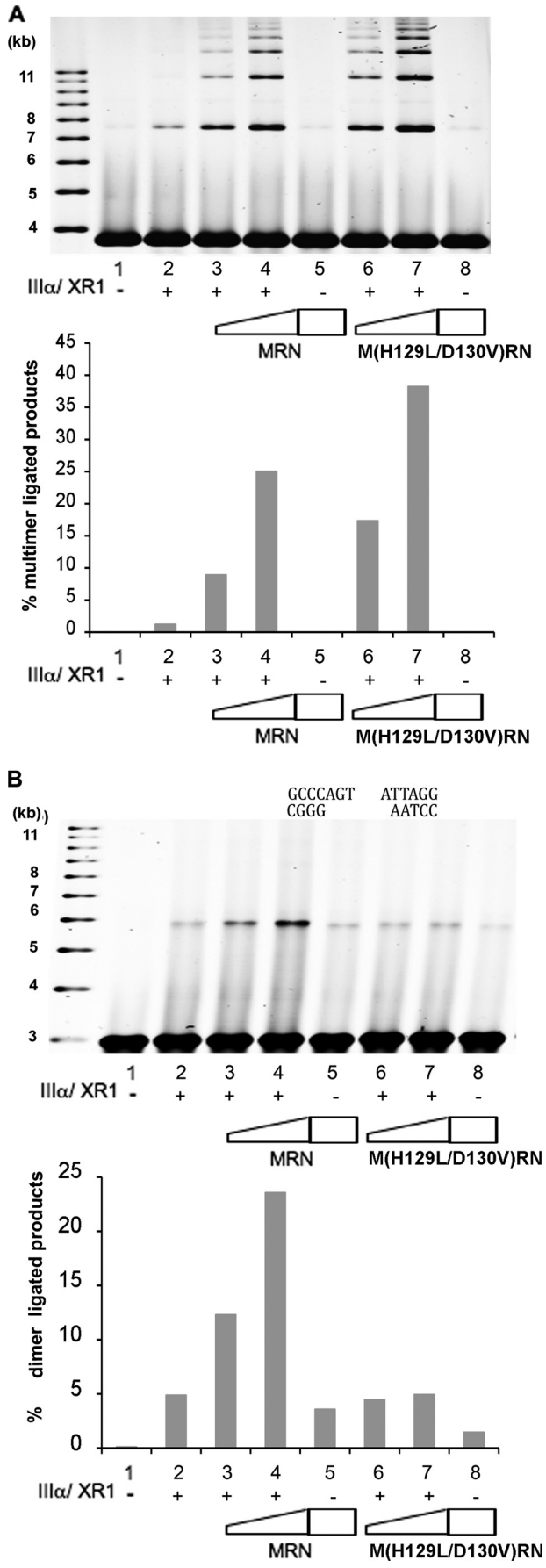

enhanced the joining of incompatible DNA ends whereas Nbs1 (Fig. 5*B*, *lanes 9* and *10*) and hMre11 (data not shown) did not.

It is likely that the end-tethering activity of MRN and MR contributes to this stimulation (45). Because these assays were carried out in the presence of Mg^{2+} and it has been shown recently that the Mre11 nuclease is active under these conditions (46, 47), it is possible that end processing by the hMre11 nuclease within the context of the MRN complex may also contribute to the increased ligation. To test this, we compared the activity of MRN complexes containing either wild-type hMre11 or a nuclease-defective version, hMre11H129L/D130V that is analogous to *Saccharomyces cerevisiae* Mre11-3 (48). Both the wild-type and mutant MRN complexes stimulated the joining of compatible DNA ends (Fig. 6*A*) whereas only the wild-type complex markedly increased joining of incompatible DNA ends (Fig. 6*B*), indicating that hMre11 nuclease activity does contribute to the joining of incompatible DNA ends.

Because hMre11 nuclease activity is stimulated by mismatched DNA ends but pauses when microhomologies are exposed (35, 49), we examined the junction sequences generated when incompatible DNA ends are joined by MRN and DNA ligase IIIα/XRCC1 using the DNA substrates and assay shown in Fig. 7*A*. These assays were carried out in the presence of Mn^{2+} to maximize hMre11 nuclease activity (50). As expected, the joining of DNA ends with incompatible 3′ overhangs was more efficient in reactions with MRN compared with hMre11 alone (Fig. 7*B*, compare *lanes 3* and *4*), suggesting that the interaction between MRN and DNA ligase IIIα/XRCC1 enhances the co-ordination of end alignment, processing, and ligation. To characterize the joining reaction further, the ligation products were amplified by PCR, cloned, and sequenced. None of the 28 ligation events generated by MRN and DNA ligase IIIα/XRCC1 that were analyzed involved degradation beyond the single-strand overhang, presumably because of the weak exonuclease activity of hMre11 on 3′ overhangs (35).

In assays using a DNA substrate with incompatible 5′ overhangs, we again observed ligation by a combination of hMre11 and DNA ligase IIIα/XRCC1 that was more efficient when hMre11 was complexed with hRad50 and Nbs1 (Fig. 7*C*). Moreover, DNA ligase IV/XRCC4 was unable to substitute for DNA ligase IIIα/XRCC1 (Fig. 7*D*, compare *lanes 4* and *5*) even though the DNA ligase complexes had similar DNA joining activity on a DNA substrate with compatible ends (supplemental Fig. S2), providing

FIGURE 6. **hMre11 nuclease activity is not required for stimulating compatible DNA end ligation but enhances incompatible DNA end ligation.** *A*, linear plasmid DNA (*lane 1*, 16 fmol) with compatible ends (PstI) was incubated with 1.4 fmol of DNA ligase IIIα/XRCC1 in the presence of no addition (*lane 2*), 312.5 fmol of wild-type MRN (*lane 3*), 625 fmol of wild-type MRN (*lane 4*), 312.5 fmol of nuclease-deficient MRN (*lane 6*), 625 fmol of nuclease-deficient MRN (*lane 7*). *Lane 5*, 625 fmol of wild-type MRN; *lane 8*, 625 fmol of nuclease-deficient MRN. DNA bands were quantified using ImageQuant TL version 2005 software, and the amount of multimeric ligated products was calculated as a percentage of the total DNA in the reaction. *B*, linear plasmid DNA (*lane 1*, 20 fmol) with incompatible, nonpalindromic ends (BglI and EcoNI) was incubated with 180 fmol of DNA ligase IIIα/XRCC1 in the presence of no addition (*lane 2*), 625 fmol of wild-type MRN (*lane 3*), 1.25 pmol of wild-type MRN (*lane 4*), 625 fmol of nuclease-deficient MRN (*lane 6*), 1.25 pmol of nuclease-deficient MRN (*lane 7*). *Lane 5*, 1.25 pmol of wild-type MRN; *lane 8*, 1.25 pmol of nuclease-deficient MRN. DNA bands were quantified, and the percentage of ligation product was calculated as a percentage of the total DNA in the reaction.

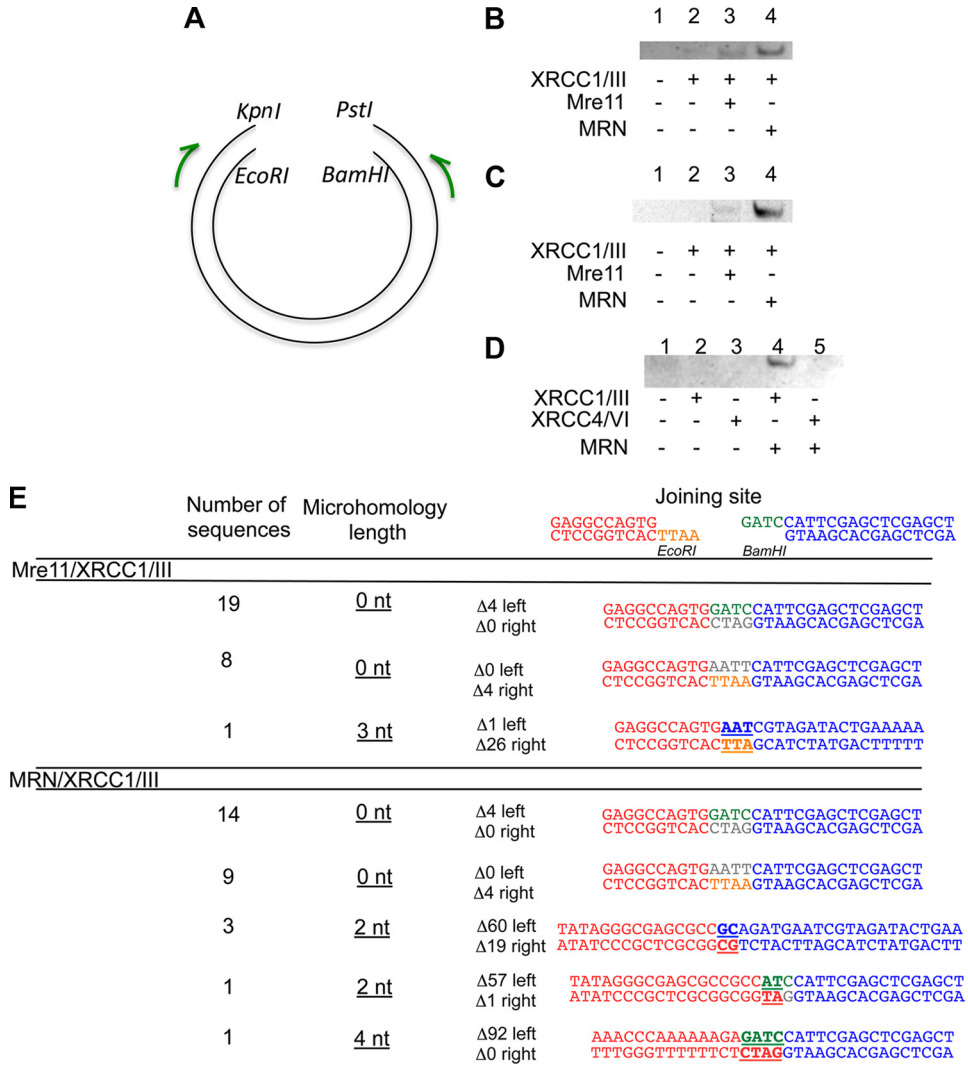

FIGURE 7. **Joining of incompatible DNA ends by MRN and DNA ligase IIIα/XRCC1: microhomology-mediated joining of DNA ends with incompatible 5′ overhangs.** *A*, circular plasmid DNA was digested with either KpnI (*left*) and PstI (*right*) to generate noncomplementary 3′ overhangs or EcoRI (*left*) and BamHI (*right*), to generate noncomplementary 5′ overhangs. Joining of the incompatible DNA ends was detected by the PCR using the indicated primers. *B*, DNA substrate (0.8 pmol) with noncomplementary 3′ overhangs was incubated with 0.01 pmol of DNA ligase IIIα/XRCC1 alone or in combination with equimolar amounts of hMre11 and MRN as indicated. *C*, DNA substrate (0.8 pmol) with noncomplementary 5′ overhangs was incubated with 0.01 pmol of DNA ligase IIIα/XRCC1 alone or in combination with equimolar amounts of hMre11 and MRN as indicated. *D*, DNA substrate (0.8 pmol) with noncomplementary 5′ overhangs was incubated with 0.01 pmol of either DNA ligase IIIα/XRCC1 or DNA ligase IV/XRCC4 in the absence or presence of an equimolar amount of MRN. *E*, sequences of the junctions generated by the joining of incompatible 5′ ends by DNA ligase IIIα/XRCC1 in combination with either hMre11 or MRN are shown. *Bolded* residues indicate microhomologies.

further evidence that the interaction between MRN and DNA ligase IIIα/XRCC1 co-ordinates end processing and ligation. Analysis of the DNA joining events by DNA sequencing revealed that the majority of the joints generated by DNA ligase IIIα/XRCC1 in conjunction with either MRN or hMre11 involved the loss of one of the 5′ single-strand overhangs (Fig. 7*E*). This may have been due to removal of one of the overhangs by hMre11 or MRN followed by ligation of the remaining overhang to the resultant blunt end. Alternatively, the mismatched 5′ ends may have been juxtaposed by hMre11 or MRN followed by ligation of one overhang to the recessed end with the other overhang forming a four-nucleotide flap. In contrast to the 3′ overhang substrate, ligations involving nucleolytic resection extending beyond the single-strand overhang for one or both of the ends were detected with the 5′ overhang substrate, presumably as a consequence of the increased activity of the hMre11 nuclease on recessed 3′ ends (35). All of the ligation events involving resection beyond the single-strand overhangs occurred at microhomologies ranging from two to four nucleotides and a higher frequency of microhomology-mediated end joining occurred when hMre11 was complexed with hRad50 (Fig. 7*E*). Thus, joining events resulting from the co-ordinated actions of MRN and DNA ligase IIIα/XRCC1 involve deletions and microhomologies that are characteristic of *in vivo* DSB repair by alt-NHEJ.

DISCUSSION

The cellular response to DSBs is complex involving DSB recognition, activation of cell cycle checkpoints, and several different DNA repair pathways. Recently, there has been growing interest in alternative versions of NHEJ pathway that appear to be distinct from the major DNA PK-dependent NHEJ pathway

(51, 52). Interestingly, repair of DSBs by alt-NHEJ is characterized by large deletions and chromosomal translocations, types of genomic rearrangements that are frequently observed in cancer cells (51, 52). A number of repair factors, including PARP-1 (17, 18, 53), MRN, (21–24), Werner syndrome protein (10), and DNA ligase IIIα/XRCC1 (10, 17, 27), have been implicated in alt-NHEJ, but the number and mechanisms of the subpathways that contribute to alt-NHEJ are poorly defined.

Here, we have identified a physical and functional interaction between MRN and DNA ligase IIIα/XRCC1 that generates repair events consistent with *in vivo* microhomology-mediated alt-NHEJ. In undamaged cells with a functional DNA PK-dependent pathway, MRN and DNA ligase IIIα/XRCC1 reside together within PML bodies. Following DNA damage, MRN and DNA ligase IIIα/XRCC1 dissociate, presumably reflecting their participation in ATM activation and end resection in conjunction with CtIP at DSBs (19, 20, 54–56) and the assembly of single-strand break repair proteins at SSBs (25), respectively.

Although alt-NHEJ is a minor back-up pathway in cells with a functional DNA PK-dependent pathway, it is more evident in cell lines defective in one or more components of the major DNA PK-dependent NHEJ pathway, suggesting that C-NEHJ suppresses alt-NHEJ and/or alt-NHEJ is up-regulated in the absence of C-NHEJ (6–9). In accord with this idea, the steady-state levels of DNA ligase IIIα were elevated in both DNA PKcs mutant and DNA ligase IV mutant cell lines. Furthermore, more DNA ligase IIIα/XRCC1 remains associated with MRN following DNA damage in DNA PK-deficient cell lines, and there is increased association between MRN and DNA ligase IIIα/XRCC1 following DNA damage in DNA ligase IV-deficient cells, suggesting that these factors participate together in the repair of DSBs by alt-NHEJ.

Our biochemical studies further support the notion that MRN and DNA ligase IIIα/XRCC1 act together in alt-NHEJ. MRN interacts with DNA ligase IIIα/XRCC1 and specifically stimulates the intermolecular joining of DNA molecules with compatible ends. This is reminiscent of the effect of yeast MRX on DNA joining by yeast Dnl4/Lif1 (43) and presumably involves both end bridging by MRN (57) and recruitment of DNA ligase IIIα/XRCC1 to the aligned DNA ends via specific protein-protein interactions. In accord with the biochemical properties of the hMre11 exonuclease (35, 49), DNA molecules with incompatible ends were resected and aligned via exposed microhomologies by MRN prior to ligation by DNA ligase IIIα/XRCC1, mimicking characteristics of *in vivo* DSB repair by alt-NHEJ. Notably, there was less joining in reactions with hMre11 compared with MRN, and DNA ligase IV/XRCC4 could not substitute for DNA ligase IIIα/XRCC1, indicating that end processing and ligation are coupled by physical and functional interactions between MRN and DNA ligase IIIα/XRCC1.

Two recent studies have shown that although DNA ligase IIIα has an essential mitochondrial function, it appears to play a less critical role than DNA ligase I in nuclear DNA repair (58, 59). Paradoxically, mouse *ligI*-null cells have no apparent DNA repair defect (60). It seems likely that there is functional redundancy between DNA ligases I and IIIα and that the extent of this redundancy may vary depending on the type of DNA damage, the cell cycle stage, and the cell type. Although our cell biology and biochemical studies describing a physical and functional interaction between MRN and DNA ligase IIIα/XRCC1 provide a molecular link between two factors implicated in alt-NHEJ, they do not exclude the possibility that there may be other subpathways of alt-NHEJ involving other DNA ligases. In support of this idea, a recent study by the Jasin laboratory provides evidence that there are both DNA ligase I- and DNA ligase IIIα-dependent alt-NHEJ subpathways (61).

Ku is a key factor in determining repair pathway choice because its binding to DSBs protects the ends from resection (62) and sequesters them into the C-NHEJ pathway (63). In the absence of either DNA PKcs or DNA ligase IV/XRCC4, Ku binding is likely to be less stable (62, 64) and the repair of DSBs much slower (7, 27). This presumably will enable other factors such as PARP-1 to gain access to the DSBs, leading to the recruitment of MRN and other factors involved in end resection (18, 20, 53). If a homologous duplex is not available, repair of the resected ends will occur by either single-strand annealing, which generates intrachromosomal deletions, or alt-NHEJ, which generates chromosomal translocations (51, 52, 65). Interestingly, cell lines established from a variety of different human malignancies are similar to the DNA ligase IV-deficient human cell lines in that they have elevated steady levels of DNA ligase IIIα and reduced steady-state levels of DNA ligase IV (10, 66). In chronic myeloid leukemia cells expressing BCR-ABL1, the overexpressed DNA ligase IIIα participates in an alt-NHEJ pathway that plays an important role in the repair of endogenous DSBs and DSBs generated by exogenous agents (10). Although it is likely that the reduced activity of C-NHEJ and increased contribution of alt-NHEJ to DSB repair in human cancers result in genome instability, in particular chromosomal translocations, that drives disease progression, the increased reliance of cancer cells on alt-NHEJ compared with normal cells suggests that inhibitors of alt-NHEJ may have therapeutic utility as they will preferentially target cancer cells.

Acknowledgments—We thank Drs. Concannon and Lieber for kindly providing human DNA ligase IV mutant cell lines and Dr. Patrick Sung for purified yeast Mre11/Rad50/Xrs2 complex.

REFERENCES

1. Venkitaraman, A. R. (2002) *Cell* **108,** 171–182
2. Ferguson, D. O., Sekiguchi, J. M., Chang, S., Frank, K. M., Gao, Y., DePinho, R. A., and Alt, F. W. (2000) *Proc. Natl. Acad. Sci. U.S.A.* **97,** 6630–6633
3. Sharpless, N. E., Ferguson, D. O., O'Hagan, R. C., Castrillon, D. H., Lee, C., Farazi, P. A., Alson, S., Fleming, J., Morton, C. C., Frank, K., Chin, L., Alt, F. W., and DePinho, R. A. (2001) *Mol. Cell* **8,** 1187–1196
4. Lieber, M. R. (2008) *J. Biol. Chem.* **283,** 1–5
5. Weterings, E., and Chen, D. J. (2008) *Cell Res.* **18,** 114–124
6. Soulas-Sprauel, P., Le Guyader, G., Rivera-Munoz, P., Abramowski, V., Olivier-Martin, C., Goujet-Zalc, C., Charneau, P., and de Villartay, J. P. (2007) *J. Exp. Med.* **204,** 1717–1727
7. Yan, C. T., Boboila, C., Souza, E. K., Franco, S., Hickernell, T. R., Murphy, M., Gumaste, S., Geyer, M., Zarrin, A. A., Manis, J. P., Rajewsky, K., and Alt, F. W. (2007) *Nature* **449,** 478–482
8. Corneo, B., Wendland, R. L., Deriano, L., Cui, X., Klein, I. A., Wong, S. Y., Arnal, S., Holub, A. J., Weller, G. R., Pancake, B. A., Shah, S., Brandt, V. L., Meek, K., and Roth, D. B. (2007) *Nature* **449,** 483–486
9. Guirouilh-Barbat, J., Rass, E., Plo, I., Bertrand, P., and Lopez, B. S. (2007)

Proc. Natl. Acad. Sci. U.S.A. **104,** 20902–20907
10. Sallmyr, A., Tomkinson, A. E., and Rassool, F. V. (2008) *Blood* **112,** 1413–1423
11. Zhu, C., Mills, K. D., Ferguson, D. O., Lee, C., Manis, J., Fleming, J., Gao, Y., Morton, C. C., and Alt, F. W. (2002) *Cell* **109,** 811–821
12. Wang, J. H., Gostissa, M., Yan, C. T., Goff, P., Hickernell, T., Hansen, E., Difilippantonio, S., Wesemann, D. R., Zarrin, A. A., Rajewsky, K., Nussenzweig, A., and Alt, F. W. (2009) *Nature* **460,** 231–236
13. Wang, J. H., Alt, F. W., Gostissa, M., Datta, A., Murphy, M., Alimzhanov, M. B., Coakley, K. M., Rajewsky, K., Manis, J. P., and Yan, C. T. (2008) *J. Exp. Med.* **205,** 3079–3090
14. Simsek, D., and Jasin, M. (2010) *Nat. Struct. Mol. Biol.* **17,** 410–416
15. Boboila, C., Jankovic, M., Yan, C. T., Wang, J. H., Wesemann, D. R., Zhang, T., Fazeli, A., Feldman, L., Nussenzweig, A., Nussenzweig, M., and Alt, F. W. (2010) *Proc. Natl. Acad. Sci. U.S.A.* **107,** 3034–3039
16. Ikejima, M., Noguchi, S., Yamashita, R., Ogura, T., Sugimura, T., Gill, D. M., and Miwa, M. (1990) *J. Biol. Chem.* **265,** 21907–21913
17. Audebert, M., Salles, B., and Calsou, P. (2004) *J. Biol. Chem.* **279,** 55117–55126
18. Wang, M., Wu, W., Wu, W., Rosidi, B., Zhang, L., Wang, H., and Iliakis, G. (2006) *Nucleic Acids Res.* **34,** 6170–6182
19. Bekker-Jensen, S., Lukas, C., Kitagawa, R., Melander, F., Kastan, M. B., Bartek, J., and Lukas, J. (2006) *J. Cell Biol.* **173,** 195–206
20. Sartori, A. A., Lukas, C., Coates, J., Mistrik, M., Fu, S., Bartek, J., Baer, R., Lukas, J., and Jackson, S. P. (2007) *Nature* **450,** 509–514
21. Deriano, L., Stracker, T. H., Baker, A., Petrini, J. H., and Roth, D. B. (2009) *Mol. Cell* **34,** 13–25
22. Dinkelmann, M., Spehalski, E., Stoneham, T., Buis, J., Wu, Y., Sekiguchi, J. M., and Ferguson, D. O. (2009) *Nat. Struct. Mol. Biol.* **16,** 808–813
23. Rass, E., Grabarz, A., Plo, I., Gautier, J., Bertrand, P., and Lopez, B. S. (2009) *Nat. Struct. Mol. Biol.* **16,** 819–824
24. Xie, A., Kwok, A., and Scully, R. (2009) *Nat. Struct. Mol. Biol.* **16,** 814–818
25. Okano, S., Lan, L., Caldecott, K. W., Mori, T., and Yasui, A. (2003) *Mol. Cell. Biol.* **23,** 3974–3981
26. Okano, S., Lan, L., Tomkinson, A. E., and Yasui, A. (2005) *Nucleic Acids Res.* **33,** 422–429
27. Wang, H., Rosidi, B., Perrault, R., Wang, M., Zhang, L., Windhofer, F., and Iliakis, G. (2005) *Cancer Res.* **65,** 4020–4030
28. Liang, L., Deng, L., Nguyen, S. C., Zhao, X., Maulion, C. D., Shao, C., and Tischfield, J. A. (2008) *Nucleic Acids Res.* **36,** 3297–3310
29. Grawunder, U., Zimmer, D., Fugmann, S., Schwarz, K., and Lieber, M. R. (1998) *Mol. Cell* **2,** 477–484
30. O'Driscoll, M., Cerosaletti, K. M., Girard, P. M., Dai, Y., Stumm, M., Kysela, B., Hirsch, B., Gennery, A., Palmer, S. E., Seidel, J., Gatti, R. A., Varon, R., Oettinger, M. A., Neitzel, H., Jeggo, P. A., and Concannon, P. (2001) *Mol. Cell* **8,** 1175–1185
31. Lees-Miller, S. P., Godbout, R., Chan, D. W., Weinfeld, M., Day, R. S., 3rd, Barron, G. M., and Allalunis-Turner, J. (1995) *Science* **267,** 1183–1185
32. Vijayakumar, S., Dziegielewska, B., Levin, D. S., Song, W., Yin, J., Yang, A., Matsumoto, Y., Bermudez, V. P., Hurwitz, J., and Tomkinson, A. E. (2009) *Mol. Cell. Biol.* **29,** 2042–2052
33. Lee, J. H., Goodarzi, A. A., Jeggo, P. A., and Paull, T. T. (2010) *EMBO J.* **29,** 574–585
34. Lee, J. H., and Paull, T. T. (2004) *Science* **304,** 93–96
35. Paull, T. T., and Gellert, M. (1998) *Mol. Cell* **1,** 969–979
36. Cheng, W. H., von Kobbe, C., Opresko, P. L., Arthur, L. M., Komatsu, K., Seidman, M. M., Carney, J. P., and Bohr, V. A. (2004) *J. Biol. Chem.* **279,** 21169–21176
37. Cahill, D., and Carney, J. P. (2007) *Mutagenesis* **22,** 269–274
38. Mackey, Z. B., Ramos, W., Levin, D. S., Walter, C. A., McCarrey, J. R., and Tomkinson, A. E. (1997) *Mol. Cell. Biol.* **17,** 989–998
39. Krejci, L., Damborsky, J., Thomsen, B., Duno, M., and Bendixen, C. (2001) *Mol. Cell. Biol.* **21,** 966–976
40. Tsuchida, R., Yamada, T., Takagi, M., Shimada, A., Ishioka, C., Katsuki, Y., Igarashi, T., Chessa, L., Delia, D., Teraoka, H., and Mizutani, S. (2002) *Radiat. Res.* **158,** 195–201
41. Stiff, T., O'Driscoll, M., Rief, N., Iwabuchi, K., Löbrich, M., and Jeggo, P. A. (2004) *Cancer Res.* **64,** 2390–2396
42. Mackey, Z. B., Niedergang, C., Murcia, J. M., Leppard, J., Au, K., Chen, J., de Murcia, G., and Tomkinson, A. E. (1999) *J. Biol. Chem.* **274,** 21679–21687
43. Chen, L., Trujillo, K., Ramos, W., Sung, P., and Tomkinson, A. E. (2001) *Mol. Cell* **8,** 1105–1115
44. Husain, I., Tomkinson, A. E., Burkhart, W. A., Moyer, M. B., Ramos, W., Mackey, Z. B., Besterman, J. M., and Chen, J. (1995) *J. Biol. Chem.* **270,** 9683–9690
45. de Jager, M., van Noort, J., van Gent, D. C., Dekker, C., Kanaar, R., and Wyman, C. (2001) *Mol. Cell* **8,** 1129–1135
46. Hopkins, B. B., and Paull, T. T. (2008) *Cell* **135,** 250–260
47. Nicolette, M. L., Lee, K., Guo, Z., Rani, M., Chow, J. M., Lee, S. E., and Paull, T. T. (2010) *Nat. Struct. Mol. Biol.* **17,** 1478–1485
48. Bressan, D. A., Olivares, H. A., Nelms, B. E., and Petrini, J. H. (1998) *Genetics* **150,** 591–600
49. Paull, T. T., and Gellert, M. (2000) *Proc. Natl. Acad. Sci. U.S.A.* **97,** 6409–6414
50. Trujillo, K. M., Yuan, S. S., Lee, E. Y., and Sung, P. (1998) *J. Biol. Chem.* **273,** 21447–21450
51. Haber, J. E. (2008) *Proc. Natl. Acad. Sci. U.S.A.* **105,** 405–406
52. Nussenzweig, A., and Nussenzweig, M. C. (2007) *Cell* **131,** 223–225
53. Brown, M. L., Franco, D., Burkle, A., and Chang, Y. (2002) *Proc. Natl. Acad. Sci. U.S.A.* **99,** 4532–4537
54. Gatei, M., Young, D., Cerosaletti, K. M., Desai-Mehta, A., Spring, K., Kozlov, S., Lavin, M. F., Gatti, R. A., Concannon, P., and Khanna, K. (2000) *Nat. Genet.* **25,** 115–119
55. Lim, D. S., Kim, S. T., Xu, B., Maser, R. S., Lin, J., Petrini, J. H., and Kastan, M. B. (2000) *Nature* **404,** 613–617
56. Zhao, S., Weng, Y. C., Yuan, S. S., Lin, Y. T., Hsu, H. C., Lin, S. C., Gerbino, E., Song, M. H., Zdzienicka, M. Z., Gatti, R. A., Shay, J. W., Ziv, Y., Shiloh, Y., and Lee, E. Y. (2000) *Nature* **405,** 473–477
57. Williams, R. S., Moncalian, G., Williams, J. S., Yamada, Y., Limbo, O., Shin, D. S., Groocock, L. M., Cahill, D., Hitomi, C., Guenther, G., Moiani, D., Carney, J. P., Russell, P., and Tainer, J. A. (2008) *Cell* **135,** 97–109
58. Gao, Y., Katyal, S., Lee, Y., Zhao, J., Rehg, J. E., Russell, H. R., and McKinnon, P. J. (2011) *Nature* **471,** 240–244
59. Simsek, D., Furda, A., Gao, Y., Artus, J., Brunet, E., Hadjantonakis, A. K., Van Houten, B., Shuman, S., McKinnon, P. J., and Jasin, M. (2011) *Nature* **471,** 245–248
60. Bentley, D. J., Harrison, C., Ketchen, A. M., Redhead, N. J., Samuel, K., Waterfall, M., Ansell, J. D., and Melton, D. W. (2002) *J. Cell Sci.* **115,** 1551–1561
61. Simsek, D., Brunet, E., Wong, S. Y., Katyal, S., Gao, Y., McKinnon, P. J., Lou, J., Zhang, L., Li, J., Rebar, E. J., Gregory, P. D., Holmes, M. C., and Jasin, M. (2011) *PLoS Genet.* **7,** e1002080
62. Zhang, Y., Hefferin, M. L., Chen, L., Shim, E. Y., Tseng, H. M., Kwon, Y., Sung, P., Lee, S. E., and Tomkinson, A. E. (2007) *Nat. Struct. Mol. Biol.* **14,** 639–646
63. Fattah, F., Lee, E. H., Weisensel, N., Wang, Y., Lichter, N., and Hendrickson, E. A. (2010) *PLoS Genet.* **6,** e1000855
64. Mari, P. O., Florea, B. I., Persengiev, S. P., Verkaik, N. S., Brüggenwirth, H. T., Modesti, M., Giglia-Mari, G., Bezstarosti, K., Demmers, J. A., Luider, T. M., Houtsmuller, A. B., and van Gent, D. C. (2006) *Proc. Natl. Acad. Sci. U.S.A.* **103,** 18597–18602
65. Lieber, M. R. (2010) *Nat. Struct. Mol. Biol.* **17,** 393–395
66. Chen, X., Zhong, S., Zhu, X., Dziegielewska, B., Ellenberger, T., Wilson, G. M., MacKerell, A. D., Jr., and Tomkinson, A. E. (2008) *Cancer Res.* **68,** 3169–3177